HOKKAIDO UNIVERSITY

Title	Strong and Tough Polyion-Complex Hydrogels from Oppositely Charged Polyelectrolytes: A Comparative Study with Polyampholyte Hydrogels
Author(s)	Luo, Feng; Sun, Tao Lin; Nakajima, Tasuku et al.
Citation	Macromolecules, 49(7), 2750-2760 https://doi.org/10.1021/acs.macromol.6b00235
Issue Date	2016-04-12
Doc URL	https://hdl.handle.net/2115/64952
Rights	This document is the Accepted Manuscript version of a Published Work that appeared in final form in Macromolecules, copyright ©2016 American Chemical Society after peer review and technical editing by the publisher. To access the final edited and published work see http://pubs.acs.org/doi/abs/10.1021/acs.macromol.6b00235
Type	journal article
File Information	Strong and Tough.pdf

Hokkaido University Collection of Scholarly and Academic Papers : HUSCAP

This document is confidential and is proprietary to the American Chemical Society and its authors. Do not copy or disclose without written permission. If you have received this item in error, notify the sender and delete all copies.

Strong and Tough Polyion-Complex Hydrogels from Oppositely Charged Polyelectrolytes: A Comparative Study with Polyampholyte Hydrogels

Journal:	*Macromolecules*
Manuscript ID	ma-2016-00235y.R1
Manuscript Type:	Article
Date Submitted by the Author:	n/a
Complete List of Authors:	Luo, Feng; Faculty of Advanced Life Science, Sun, Tao Lin; Hokkaido University, Graduate School of Science Nakajima, Tasuku; Hokkaido University, Faculty of Advanced Life Science King, Daniel; Hokkaido University, Faculty of Advanced Life Science Kurokawa, Takayuki; Faculty of Advanced Life Science, Hokkaido University Zhao, Yu; Graduate School of Life Science, Hokkaido University Ihsan, Abu Bin; Hokkaido University, Graduate School of Science Li, Xufeng; Hokkaido University, Guo, Honglei ; Graduate School of Life Science, Hokkaido University Gong, Jian Ping; Hokkaido University, Graduate School of Science

SCHOLARONE™
Manuscripts

Strong and Tough Polyion-Complex Hydrogels from Oppositely Charged Polyelectrolytes: A Comparative Study with Polyampholyte Hydrogels

Feng Luo[1,$], Tao Lin Sun[1,2], Tasuku Nakajima[1,2], Daniel R. King[1,2], Takayuki Kurokawa[1,2], Yu Zhao[3], Abu Bin Ihsan[1], Xufeng Li[3], Honglei Guo[3], Jian Ping Gong[1,2*]

[1]*Faculty of Advanced Life Science, Hokkaido University, Sapporo 060-0810, Japan*

[2]*Global Station for Soft Matter, Global Institution for Collaborative Research and Education, Hokkaido University, Sapporo, Japan*

[3]*Graduate School of Life Science, Hokkaido University, Sapporo 060-0810, Japan*

*Corresponding author: gong@mail.sci.hokudai.ac.jp

$: Present Address

F．Luo: College of Polymer Science and Engineering, State Key Laboratory of Polymer Materials Engineering, Sichuan University, Chengdu 610065, China

Abstract

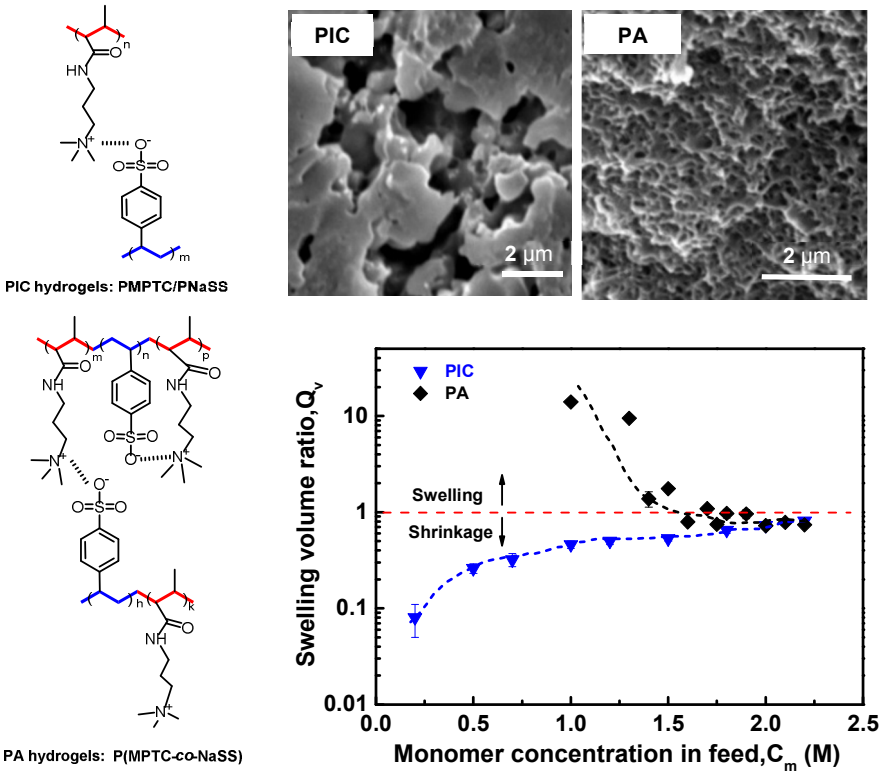
Oppositely charged homo-polyelectrolytes were found to form strong, tough, and self-healing polyion-complex (PIC) hydrogels, in similar to polyampholytes (PA) that have opposite charges randomly distributed on the same polymer chains. The excellent mechanical performances of these two novel hydrogels are the results of dynamic ionic bonds formation between entangled polymer chains. For PIC system, only inter-chain bonding occurs, while for PA system both inter- and intra-chain bonding exist. In addition, the ion pairs are expected to form stronger bonding in PIC system than those in PA system. In this work, we performed a comparative study of PIC hydrogels with the PA hydrogels. The PIC hydrogels are synthesized by sequential homo-polymerization of

cationic and anionic monomers at varied formulation, and their swelling and mechanical properties are systematically studied in comparison to the PA hydrogels that were synthesized from random copolymerization of anionic monomers and cationic monomers of the similar formulation. Different from the PA system that only forms tough hydrogels around zero-net charge composition without chemical cross-linking, the PIC system forms tough physical hydrogels even at weakly off-balanced charge composition. At the charge-balanced composition, the low entanglement concentration of homo-charged polyelectrolyte chains leads to tough PIC hydrogels formation at much lower concentrations than that of PA hydrogels. As a result, the PIC hydrogels are much tougher than the PA hydrogels prepared at the same monomer composition. In similar to PA hydrogels, the PIC hydrogels also exhibit broad dynamic mechanical spectra, indicating the formation of ion complexes with widely ranged bond strength. The PIC hydrogels have strong viscoelasticity in comparison with PA hydrogels. However, the two systems show the similar activation energies of the dynamic mechanical spectra. The SEM microstructural observation shows that the PIC hydrogels have segregated structure while PA hydrogels are more homogeneous.

for Table of Contents use only

Strong and Tough Polyion-Complex Hydrogels from Oppositely Charged Polyelectrolytes: A Comparative Study with Polyampholyte Hydrogels

Feng Luo[1,$], Tao Lin Sun[1,2], Tasuku Nakajima[1,2], Daniel R. King[1,2], Takayuki Kurokawa[1,2], Yu Zhao[3], Abu Bin Ihsan[1], Xufeng Li[3], Honglei Guo[3] and Jian Ping Gong[1,2*]



1. Introduction

Hydrogels are "soft and wet" materials that possess unique properties necessary for application in biomaterials, soft robotics, smart actuators, and sensors.[1-8] The applicability of hydrogels, however, is often severely limited by their weak and brittle mechanical properties, which are due to intrinsic structural inhomogeneity and lack of an effective energy dissipation mechanism. Therefore, developing robust hydrogels with excellent mechanical properties and functionality has long been pursued by material scientists. In nature, tough and strong hydrogels, like natural, load-bearing soft tissues such as tendon, cartilage, muscle, and blood vessels, have been used to inspire soft materials design. During the past few decades, much effort has been devoted to developing tough hydrogels, such as double-network hydrogels,[9] nanocomposite hydrogels,[10-11] hybrid hydrogels[8, 12-13] , and others.[14-15] Among them, the double network (DN) strategy has been shown to be extraordinarily effective in improving the toughness of hydrogels, and the "sacrificial bond" mechanism was shown to efficiently dissipate energy.[16] Since the rupture of covalent bonds in traditional DN gels is irreversible, DN gels exhibit permanent softening after large deformation, which is a limitation in many practical applications. To address this problem, physically reversible bonds can be built in the hydrogel as a renewable "sacrificial bond" to replace the irreversible covalent bonds. Hydrogen bonds,[17] metal–ligand interactions,[18] ionic bonds,[19-20] charge-driven self-assembling,[21-23] Van der Waals interactions,[24] π-π interactions,[25] and hydrophobic interactions,[26] are all potential candidates as a renewable "sacrificial bond." Studies along these lines have successfully produced tough double network hydrogels with self-recovery after internal rupture.[1, 19, 27]

The double network concept, incorporating a mechanically fragile structure to toughen the entire material, suggests a more general strategy of incorporating dynamic physical bonds for developing tough hydrogels. Recently, our group developed two kinds of robust and self-healing physical hydrogels using dynamic ionic bonds. One is polyampholyte (PA) hydrogels from one-step free radical copolymerization of charge-balanced anionic and cationic monomers.[28-30] Another is polyion-complex (PIC) hydrogels from sequential homopolymerization of opposite charged cationic and anionic monomers. [31-32] In these gels, dynamic ionic bonds, of wide distribution in strength, are formed. The strong bonds serve as crosslinkers, imparting elasticity, whereas the weak bonds serve as reversible sacrificial bonds, imparting toughness and self-healing.

Considering that both PIC hydrogels and PA hydrogels are formed from oppositely charged monomers but with different primary structures of polymers through different synthesizing processes, it is interesting to compare the behaviors of these two systems. For example, both inter- and intra-chain bonding exist in the PA system, while PIC system only has inter-chain bonding. How does this difference influence the stability of the ionic bond strength? In the case of PA hydrogels, the primary structure of the polymer strongly depends on the reactivity ratios of the two oppositely charged monomers, which makes it a complex system to reveal the detailed correlation between the structure and the properties of these gels. In contrast, PIC hydrogels, consisting of oppositely charged homo-polymers, are relatively simple to study. By comparing the behaviors of the two systems, we might obtain insight to understand the PA system.

Previous studies have shown that the charge ratio and the monomer concentration are two important factors influencing PA hydrogel structure and properties.[28, 30] In this

work, we systematically study the effects of charge ratio, the monomer concentrations, and the molecular weight of polyelectrolytes on the swelling, dynamic mechanical response, and mechanical performance of PIC hydrogels via a comparative study with PA hydrogels synthesized from the same pair of cationic and anionic monomers.

2. Experimental section

2.1 Materials

Commercially available anionic monomer, sodium *p*-styrenesulfonate (NaSS); cationic monomer, 3-(methacryloylamino)propyl-trimethylammonium chloride (MPTC); UV initiator, α-ketoglutaric acid; and NaCl are all purchased from Wako Pure Chemical Industries, Ltd. and used as received. Millipore de-ionized water is used in all of the experiments.

2.2 Synthesis of hydrogels

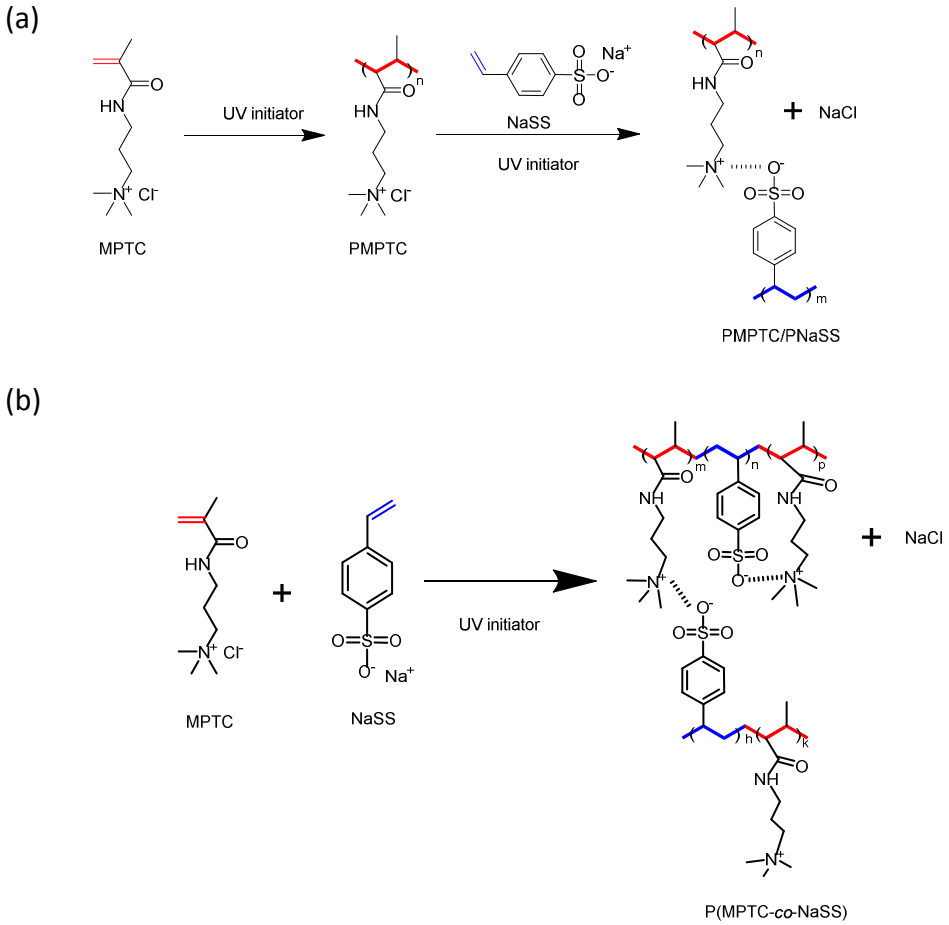
Polyion complex hydrogels. The PIC hydrogel was synthesized by sequential homo-polymerization of cationic and anionic monomers, as shown in Scheme 1a, which is the same method as that employed in the previous report.[31] Typically, the sample is referred to as PM_1/PM_2 (C_m-f-x_1-x_2), where P is the abbreviation of poly-, and M_i, (i = 1,2) is the abbreviated monomer name in the *ith* step of the polymerization. C_m is the overall molar concentration at the second component polymerization, f is the molar fraction of anionic monomer, and x_1 and x_2 are initiator concentrations of the first and second polymerization (mol%), relative to the corresponding monomers. For example, to synthesize the PMPTC/PNaSS(1.5-0.5-0.05-0.1) hydrogel, PMPTC was first synthesized from an aqueous solution of 1 M MPTC containing x_1=0.05 mol-% initiator, 2-oxoglutaric acid, by UV light irradiation (light intensity ~ 4 mW/cm^2) for 8 h. The produced PMPTC was dried and made into a powder. Next the powder was mixed with NaSS monomer with the charge fraction of the second monomer NaSS, f =[NaSS]/([MPTC]+ [NaSS])=0.5. After well dispersion with 0.5 M NaCl to form a

mixed solution of C_m=[MPTC]+[NaSS]=1.5 M at 60 °C, the mixture containing x_2=0.1 mol-% initiator relative to the second monomer was polymerized under UV light for 8 h in a reaction cell consisting of a pair of glass plates with 1.5 mm spacing. The as-prepared hydrogel was then dialyzed in a large amount of water to remove the mobile counter ions and co-ions from the product. After dialysis, the opposite charges on the polymer chains formed ion bonds. Thus, the thickness of the sample shrank and the equilibrium hydrogel was obtained. Different C_m from 0.2 to 2.2 M and different molar fractions *f* from 0.45 to 0.55 were investigated in this work.

Polyampholyte hydrogels. PA hydrogels P(MPTC-*co*-NaSS), synthesized from random copolymerization of anionic monomer NaSS and cationic monomer MPTC, as shown in Scheme 1b, was obtained according to our previous report.[28,29, 33] The mixed solution with prescribed total ionic monomer concentration C_m, molar fraction of anionic monomer *f*, 0.25mol % initiator relative to C_m was polymerized in a reaction cell with 2 mm spacing under UV light for 8 h. To reach the equilibrated state, the as-prepared gels were also immersed in a large amount of water for one week, where the mobile counter ions and unreacted co-ions were dialysed from the sample. As the PA can only form physical hydrogels in a very narrow range of *f*~0.5, the sample series with varied charge fraction *f* were synthesized in the presence of chemical cross-linker, N, N'-methylenebis(acrylamide) (MBAA) (4 mol% in relative to monomer concentration C_m). The PA sample is referred to as P(MPTC-*co*-NaSS) (C_m-*f*-C_{MBAA}), where C_m is the overall molar concentration of monomer, *f* is the molar fraction of anionic monomer, C_{MBAA} is the chemical cross-linker density. For PA hydrogels without chemical cross-linker, the sample is referred to as P(MPTC-*co*-NaSS) (C_m-*f*).

The measured reactive ratio of NaSS and MPTC is 1.48 and 0.70, respectively. [28] So the sequence of the P(MPTC-*co*-NaSS) synthesized at balanced charge composition can be

calculated as NaSS rich at the starting end of the chain and the MPTC rich at the finishing end of the chain. Also, some copolymers may not be neutral and those formed at the early stage is NaSS rich, while those at the later stage is MPTC rich. At the equilibrated state, the NaSS rich segments and MPTC rich segments would form the strong ionic complex structure as well as the entanglements, while other parts lead to the weak ionic complex. Therefore, it shows wide distribution of strong bonds and weak bonds. The strong bonds serve as permanent crosslinks, imparting the elasticity, while the weak bonds reversibly break and re-form, serving as reversible sacrificial bonds.



Scheme 1. Schematics of the preparation of the physical hydrogels by ionic bonds formation from oppositely charged homo-polyelectrolytes to form polyion-complex (PIC)

or from polyampholytes (PA) that carrying opposite charges on the same polymer chain. (a) PIC hydrogel formation: Cationic monomer (MPTC) was homopolymerized in the first step and then mix with the anionic monomer (NaSS). After mixing, the latter monomer was polymerized in the second step to form the as-prepared PIC hydrogel. By equilibrating the sample in water, small counter-ions and co-ions of the polymer are removed from the sample. As a result, tough PIC hydrogel is formed, named PMPTC/PNaSS. (b) PA hydrogel P(MPTC-*co*-NaSS) formation: synthesized from one-step random copolymerization of cationic monomer MPTC and anionic monomer NaSS.

2.3 Characterization

Swelling measurements. The swelling volume ratio, Q_v, was defined as the ratio of the sample volume at swelling equilibrium, V, to that of the as-prepared state, V_0, $Q_v = V/V_0$. The polymer molar concentration, C_p, at equilibrium of the sample was estimated from C_m/Q_v. To achieve adequate precision, three measurements were carried out on samples of different volumes taken from the same gel. The water content of dialyzed samples was measured using a moisture tester.

Tensile test. The tensile tests were carried out on dumbbell-shaped samples with the standard JIS-K6251-7 size using a commercial tensile tester (Tensilon RTC-1310A, Orientec Co.). The initial distance L_0 between the two clamps of the tester was 12 mm and the tensile deformation was performed at a series of extension rates, v, from 1 to 100 mm/min., which gives the strain rate $\dot{\varepsilon} = v/L_0$ from 0.0014 to 0.14 s^{-1}. The nominal stress, σ, was estimated from the load divided by the cross-sectional area of the undeformed sample. The strain ε was estimated from the clamp displacement divided by L_0. The

Young's modulus, *E,* was estimated as the slope of the stress-strain curve within a strain range of ε=0.03-0.1. The yield stress, $\sigma_{y,}$ was obtained at which the tangent modulus $d\sigma/d\varepsilon$ changes at the greatest rate with respect to increasing strain. The values of all the mechanical properties were calculated as averages for at least three specimens. All of the measurements were performed in air at a room temperature of about 25 °C.

Rheometry. Rheological tests were performed using an ARES rheometer (advanced rheometric expansion system, Rheometric Scientific Inc.). A rheological frequency sweep from 0.0628 to 100 rad/s was performed with a shear strain of 0.5% in the parallel-plate geometry with a temperature range of 0–90°C. The disc-shaped samples with thicknesses of ~ 1 mm and diameters of 15 mm were adhered to the plates with superglue (Aron alpha, Konishi, Japan) and surrounded by water to maintain hydration.

Scanning electron microscopy (SEM). The structure of the gels was observed by SEM (JSM-6010LA, JEOL, JAPAN) with an accelerating voltage of 20 kV. The sample gel specimens were prepared by freeze-drying the swollen gel to avoid shrinkage in the drying process. The sample was cryogenically fractured in liquid nitrogen. Before SEM characterization, the surface was treated with a thin layer of gold by sputtering method.

GPC Analysis. Molecular weights (M_w) of PMPTC were determined by GPC measurement using a HITACHI L-7110 pump and a HITACHI 7490 RI detector, using a method the same as in a previous study[34] with a slight modification: a buffer solution of 0.3M Na_2SO_4 was used as an eluent at 40 °C, and flow rate was 0.4 mL/min.

3. Results and discussion

3.1 Effects of charge fraction, monomer concentration, and molecular weight on the properties of polyion-complex hydrogels

3.1.1 Charge fraction

Polyion-complex (PIC) hydrogels are crosslinked by inter-polymer ionic bonds, and therefore the charge ratio in feed between the two oppositely charged monomers dramatically influences the resulting polymer properties. Figure 1 presents the effect of the in feed molar fraction of the second monomer NaSS, f, on the swelling volume ratio, Q_v, and the work of extension, W_b, of the PMPTC/PNaSS(1.5-f-0.05-0.1) PIC hydrogels. In a relatively wide composition range (f = 0.45 ~ 0.55) investigated, stable physical gels are formed without the presence of any chemical cross-linker. Near the charge balance point (f = 0.49 ~ 0.52), the gels shrink in water (Q_v < 1) relative to their as-prepared state, indicating that the Coulombic attraction between chains prevails over the repulsion between monomer units and the polymer chains collapse. In regions with sufficient charge imbalance (f < 0.49 or f > 0.52), on the other hand, the gels swell (Q_v > 1), indicating that the Coulombic repulsion prevails and the unpaired ion-contain segments preferentially interact with water, resulting in polymer elongation. The shrinking of the gels around the charge balance point is accompanied by a dramatic increase in the work of extension, W_b, while the swelling samples are very weak (data not shown). Thus, the optimized f value of the feed, at which Q_v reaches a minimum and W_b reaches a maximum, is almost at 0.5, which is the charge balance point. The true charge ratio, f_{true}, of PMPTC/PNaSS(1.5-f-0.05-0.1) was studied using elemental analysis (Table 1). The results revealed that best molar fraction f = 0.5 in feed also yields f_{true} =0.5, which is at

the ideal stoichiometric ratio of 1:1. It indicates that in this PIC hydrogel, complete charge balance (f_{true} = 0.5) results in the most stable state.

In the case of PA system, however, stable physical gels can only be formed around the charge balanced composition (f~0.5). Deviation from this composition gives extremely weak gels or polymer solution. For comparison, we show the behaviors of chemically crosslinked PA hydrogels P(MPTC-*co*-NaSS) 0.875-*f*-4 obtained from the previous work in Figure 1b. [28,33] The PA hydrogels also present the largest shrinkage and highest work of extension at the ideal stoichiometric ratio. In the following work, we focus our study on the physical PIC and PA hydrogels with charge balanced composition f = 0.5.

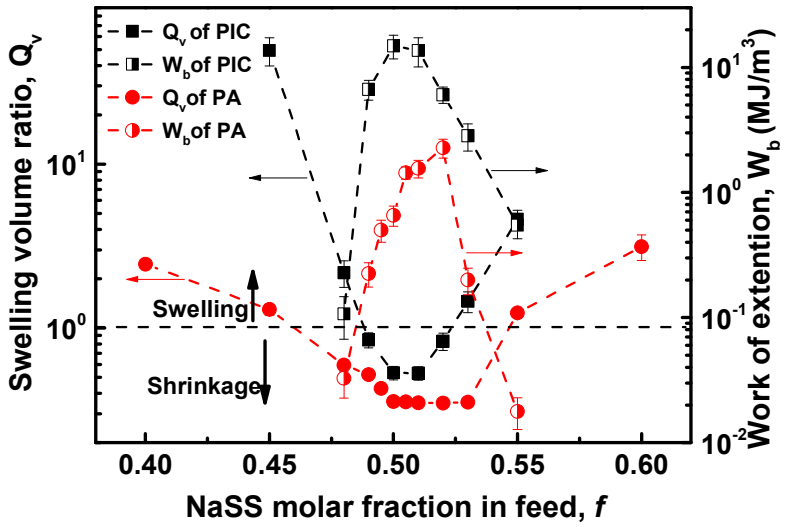


Figure 1. NaSS molar fraction (f) effects on the swelling volume ratio in relative to the as-prepared state, Q_v, and the work of extension, W_b, of the PIC hydrogels PMPTC/PNaSS(1.5-*f*-0.05-0.1). Without chemical crosslinking, the PA system can only form physical gels near the charge balanced composition (f~0.5). For comparison, the behaviors of chemically crosslinked PA hydrogels P(MPTC-*co*-NaSS) 0.875-*f*-4 are also shown. The data of P(MPTC-*co*-NaSS) hydrogels are cited from ref. 28

Table 1 The weight percentage of elements in various PIC hydrogels PMPTC/PNaSS(1.5-*f*-0.05-0.1) determined by element analysis.

f^*	C (wt %)	H (wt %)	N (wt %)	S (wt %)	Cl (wt %)	f_{true}^{**}
0.49	54.73	7.97	7.42	7.79	0.32	0.478
0.50	55.89	8.04	7.27	8.33	0	0.500
0.51	55.59	7.87	7.11	8.47	0	0.510
0.52	55.63	7.87	7.07	8.55	0	0.514

$^*f$: the charge fraction of NaSS in feed. $^{**}f_{true}$: the true charge fraction of NaSS in gel determined by element analysis.

3.1.2 Effect of monomer concentration

The mechanical properties of the PIC gels are strongly related to the concentration of monomer during preparation. Figure 2a shows the images of as-prepared PIC samples of PMPTC/PNaSS (C_m-0.5-0.05-0.1) polymerized with different total monomer concentration, C_m, from 0.2 M to 2.2 M. All of the as-prepared samples are a white, opaque gel. When the C_m is as low as 0.2 M, a thin free water layer appears on the surface of the gel. This indicates that the lowest monomer concentration required to form a non-phase-separated gel is around 0.2 M. In contrast, when the C_m is above 2.2 M, the viscosity of the mixture at the second polymerization stage becomes too high to dissolve the components.

As shown in Figure 2b, when these as-prepared PIC gels are dialyzed in water, they all shrink. The lower the in feed monomer concentration C_m, the larger the shrinkage. The shrinking volume ratio, Q_v, changes from 0.1 to 0.8 when C_m increases from 0.2 M to 2.2

M. These shrinkage behaviors of PIC hydrogels with respect to C_m are very different from that of the PA hydrogels. The PA samples of P(MPTC-co-NaSS) (C_m-0.52) show the low critical concentration for forming hydrogel at C_m =1.3 M, much higher than that of PIC system of 0.2 M.[28] Furthermore, the PA gels swell ($Q_v > 1$) at $C_m < 1.6$ M and shrink ($Q_v < 1$) at $C_m > 1.6$ M, reaching a constant Q_v value at high C_m, as also shown in Figure 2b.[28,33]. It is interesting to observe that the Q_v values of PIC and PA almost overlap at high C_m region.

On the basis of C_m and Q_v, the resulting polymer concentration at equilibrium can be estimated from $C_p = C_m/Q_v$. In the case of PIC, C_p is approximately constant of 2.5 M, independent of the initial monomer concentration in feed C_m, as shown in Figure 2b. The water content measurement also confirmed that PIC samples of C_m from 0.2 M to 2.2 M have the almost identical water content around 50~55 wt%. On the other hand, the C_p of PA samples gradually increases with C_m and reaches 2.9 M at high C_m=2.2 M, corresponding to a water content of 60 wt%. It is surprise, that the water content of the PIC gels (50~55 wt%) is very close to but slightly lower than that of PA gels prepared at high monomer concentration (C_m=2.2 M). [28,33] This indicates that the overall ionic bonds packing density of the PIC system is independent of the C_m and is slightly lower than the PA prepared at high concentration.

The correlations between the modulus E measured after dialysis and C_m are shown in Figure 2c. The PIC samples, having the constant C_p, show almost constant modulus, E, for C_m =0.2 M ~ 1.5 M, and the E slightly decreases when $C_m > 1.5$ M (Figure 2c). On the other hand, the PA samples, of which C_p increases with C_m, show increases of E with C_m and then the E saturates to the value of PIC at $C_m > 1.6$ M.

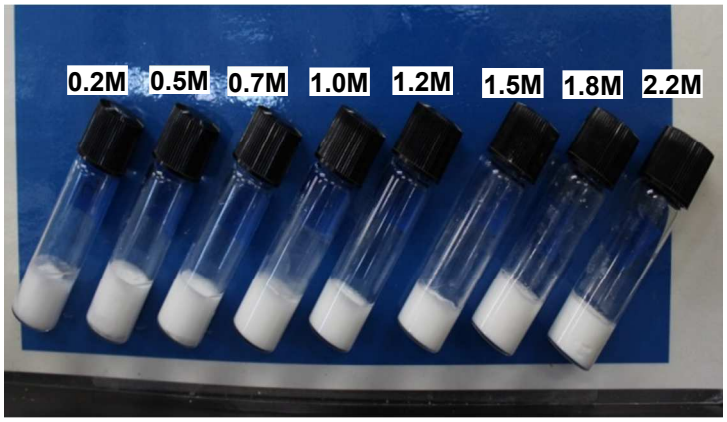
The above results indicate that PIC system have stronger ionic bond forming ability than the PA system. The different C_m effects on the volume change Q_v and therefore on the polymer concentration C_p of the gels for PIC and PA systems should be attributed to their differences in polymer chain conformation. For the PIC system, the polymer chains, carrying homo-charges, are in relatively extended conformation before complexation, which favors the inter-chain ion bonds formation even at relatively low concentration; while the PA chains, carrying opposite charges in each single chain, are in compact conformation due to intra-chain ionic bond formation, which requires very high concentration to form inter-chain bonding. This explains why the PIC system has a much lower critical concentration to form supramolecular gels than that of the PA system.

Even though the polymer concentration C_p and modulus E show weak dependence on the preparation concentration C_m, the tensile properties of PIC gels do show a strong dependence on C_m as shown in Figure 2d. In similar to the modulus, the yielding stress are also almost the same for C_m =0.2~ 1.5 M, but it becomes small when C_m > 1.5 M. The differences in initial monomer concentration also induce significant distinction in elongation at break (Figure 2d). When C_m < 0.7 M, the samples are relatively weak and fail under low strain and stress. The elongation at break of the sample with C_m =0.2 is only 1.8, while it is up to 9.0 for the sample with C_m =2.0. The C_m dependence of the fracture strain indicates the effect of trapped topological entanglement on the tensile behaviors. Generally, the entanglement density of the polymer chains increases with the concentration in a power law relation as $\sim C_m^{2.3}$.[35] The low concentration (C_m < 0.7 M) results in weak entanglement, and therefore low strain-at-break when undergoing extension. When $C_m \geq$ 0.7 M, the fracture strain becomes large and does not show

systematic dependence on C_m, which indicates that the polymer chains have strong entanglement to sustain large elongation, and the fracture is due to breaking of covalent bonds. The slight decrease in Young's modulus and yielding stress of samples, and slight increase in the fracture strain for samples prepared at C_m > 1.5 M suggest that at extremely high concentration the ionic interaction is weakened, probably by self-screen effect.

Therefore, for the PIC hydrogels, the work of extension, W_b, a quantity for assessment of toughness, increases with C_m at C_m < 0.7 M and the largest values of W_b are obtained for samples with C_m ranging from 0.7 M to 1.5 M; W_b slightly decreases with increasing C_m when C_m > 1.5 M (Figure 2e). Particularly, the W_b increases from 1.9 MJ/m^3 to 14.6 MJ/m^3 for C_m =0.2 and C_m =1.6, respectively. In contrast, the PA samples monotonously increase the mechanical toughness W_b with the increase in C_m, indicating that the entanglement effect dominates the tensile behaviors for the whole C_m range investigated. [28,33] At the optimized condition, the PIC gels show about two times of yielding stress, fracture stress but similar fracture strain in comparison with those of PA gels prepared at the highest concentration investigated C_m=2.2 M. [28,33] Thus, W_b of optimized PIC is about two times of that of PA (C_m=2.2 M) as shown in Figure 2e.

(a)



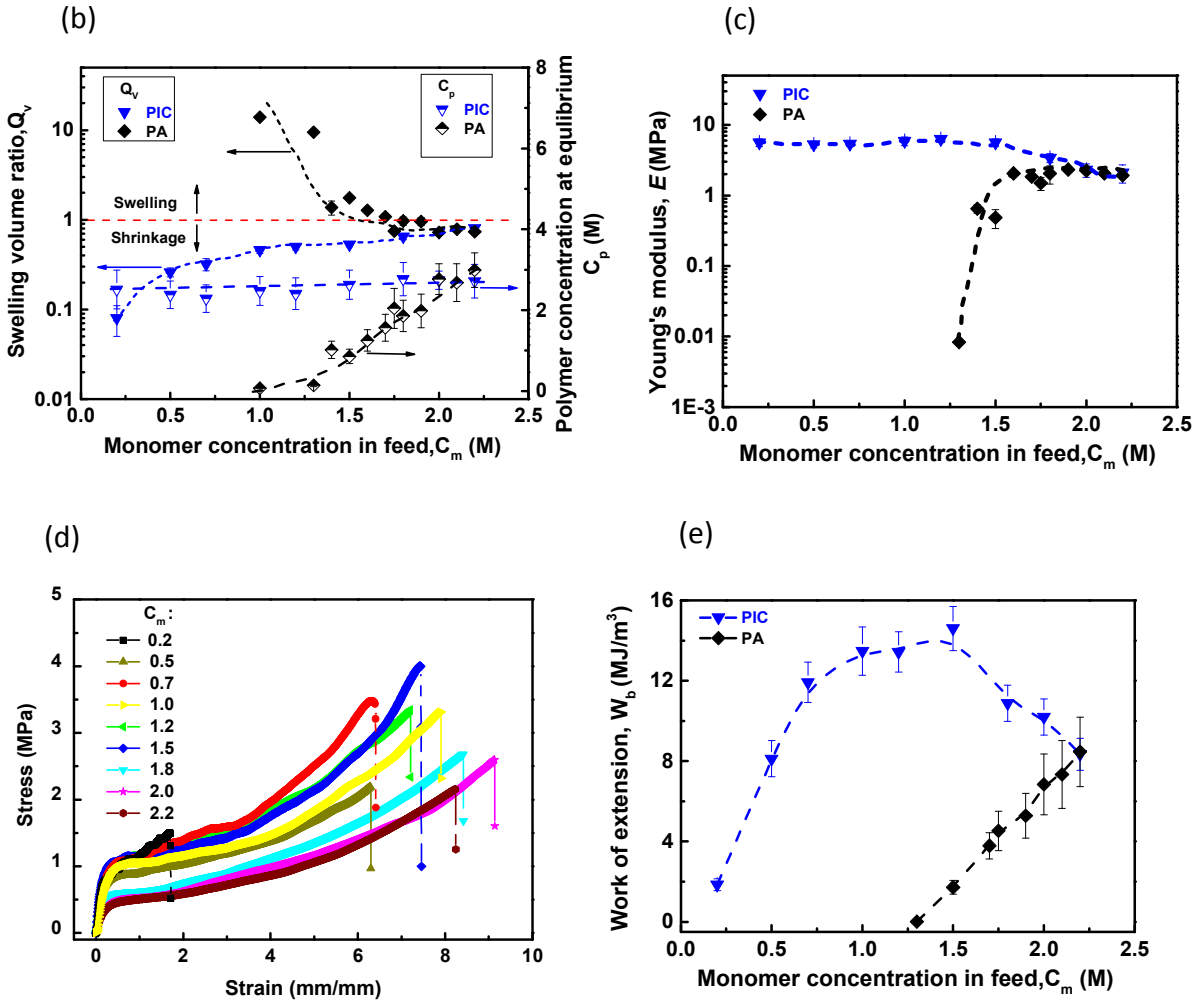


Figure 2. Effect of monomer concentration on the physical properties of PIC hydrogels. (a) Photographs of the PMPTC/PNaSS(C_m-0.5-0.05-0.1) hydrogels polymerized with different total monomer concentration in feed, C_m. Data in the figure are C_m in unit of M. (b) The C_m dependence of the volume ratio, Q_v, of the dialysed sample to the as-prepared sample, and of the polymer concentration, $C_p = C_m/Q_v$, of the dialysed sample. (c) The C_m dependence of Young's modulus (E). (d) Representative stress-strain curves of PIC hydrogels with different C_m. (e) The C_m dependence of work of extension, W_b. For comparison, the behaviors of PA hydrogels P(MPTC-*co*-NaSS) (C_m-0.52) are also shown in (b), (c), (e). Both PIC and PA hydrogels were prepared at the compositions to form

charge balanced samples. The data of PA hydrogels P(MPTC-*co*-NaSS) are cited from ref. 28 and ref. 33.

3.1.3 Molecular weight

The molecular weight of PMPTC of the PIC hydrogels discussed in the above section was measured as ~10^6 g/mol (Table 2), approximately equivalent to that of copolymer in PA hydrogel (around ~10^6 g/mol) in our previous report.[28] For radical polymerization, the molecular weight is strongly dependent on the initiator concentration for polymerization at fixed monomer concentrations. As shown in Table 2, the molecular weight of the PMPTC decreases with increasing initiator concentration in monomer solution. Specifically, the M_w of PMPTC polymerized by 0.05 mol% initiator is 3 times of that of PMPTC polymerized by 0.5 mol% initiator. As PNaSS polymerized at the second step was tightly bonded with the PMPTC by ionic bonds, we could not measure the molecular weight of the PNaSS in the PIC gels. The molecular weight of PNaSS should also decrease with increasing initiator concentration. The molecular weight effect of the PMPTC and PNaSS on the mechanical properties of the PIC hydrogels is studied. Figure 3a shows that the PIC hydrogels, PMPTC/PNaSS(1.5-0.5-x_1-0.1), composed of PMPTC polymerized with low initiator concentration have higher yielding stress and fracture energy than that of the hydrogels composed of PMPTC polymerized with high initiator concentration, while the fracture strain is almost independent of the initiator concentration. Similar results are observed for the PIC hydrogels, PMPTC/PNaSS(1.5-0.5-0.05-x_2), composed of PNaSS synthesized with different initiator concentrations x_2 (mol%) at the second step of polymerization, as shown in Figure 3b. Combining the

results of Table 2 and Figure 3, we know that the higher the molecular weight of the polymers, the higher the modulus, the yielding stress, and the toughness of the PIC hydrogels, either for the first or the second polymers. Since the yielding stress and fracture stress depend on the molecular weight while the fracture strain does not, this molecular weight effect suggests that the ionic bonds are stabilized by the increased entanglement. This phenomenon is similar to the case of adding the chemical crosslinker, which also stabilizes the ionic bonds.[30]

Table 2. Molecular weight of PMPTC-x_1 measured by GPC. Here, x_1 (mol%) *is* initiator concentration relative to the monomer MPTC.

PMPTC-x_1	Mn (g/mol)	Mw (g/mol)	Mw/Mn
PMPTC-0.05	3.75×10^6	4.66×10^6	1.24
PMPTC-0.1	9.45×10^5	2.11×10^6	2.24
PMPTC-0.5	5.81×10^5	1.49×10^6	2.57

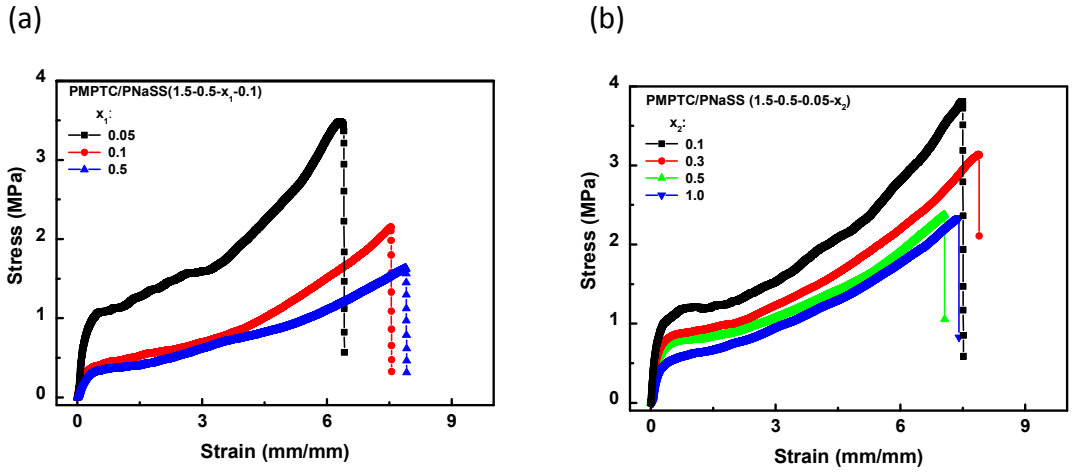


Figure 3. (a) Stress-strain curves of PMPTC/PNaSS(1.5-0.5-x_1-0.1) hydrogels with different initiator concentrations x_1 (mol%) at the first step of polymerization. (b) Stress-

strain curves of PMPTC/PNaSS(1.5-0.5-0.05-x_2) hydrogels with different initiator concentrations x_2 (mol%) at the second step of polymerization.

3.2 Structure analysis of PIC hydrogels by rheology

We have analysed the structure of the PIC hydrogels by rheology that is an effective way to study the morphology of the system. Figure 4a shows the result of a dynamic temperature sweep for PMPTC/PNaSS(1.5-0.5-0.05-0.1). The thermal energy causes the rupture of ion bonds and increases the dynamics of polymer segments, therefore, the storage modulus (G') and the loss modulus (G'') decrease about two orders of magnitude upon heating from 0 °*C* to 75 °*C* and then level off above 75 °*C*. The tanδ curve exhibits a main peak at 51 ℃ and a broad shoulder peak at 27 °*C*, suggesting that some micro phase separation structure might exist in the PIC hydrogel to form the ionic bonds of different strength. For samples at C_m =1.2 M and 2.0 M, the $G'$and G'' also decrease with increasing temperature which are similar to the tendency of C_m =1.5 M (curves are not shown). With increasing monomer concentration C_m, the intensity of tanδ decreases, and the main peak of tanδ shifts to lower temperature, as shown in Figure 4b. For hydrogels synthesized from C_m = 2.0 M, the peak at low temperature becomes the main peak. This indicates that at high concentrations that poor dispersion occurs, the formation of relatively strong ion bonds is suppressed, resulting in a majority of weak bonds. This result is in agreement with the decrease of the modulus when C_m > 1.5 M (Figure 2c).

The dynamic behaviors of the PIC hydrogels at different temperatures and frequencies well follow the principle of time-temperature superposition. Figure 4c shows the master curves of G', G'', and tanδ for the PMPTC/PNaSS(1.5-0.5-0.05-0.1) hydrogel at a

reference temperature of 20 ℃. For comparison, the corresponding master curves of P(MPTC-*co*-NaSS) (2.1-0.52) hydrogel are also shown in Figure 4c. For both PIC gel and PA gel, G' is larger than G'' over the whole frequency range from 10^{-7} to 10^{6} rad/s, indicating that both gels, even without any chemical cross-linking, are always in the gel state with predominantly elastic properties. The PIC gel shows a main peak and a broad sub-peak at frequencies around 5×10^{-3} rad/s and 1 rad/s, respectively, in its tanδ relaxation curve. This result agrees with the results of the temperature sweep that suggest the micro phase separated structure of PIC hydrogels to give a wide range of ion bond strengths. On the other hand, only one broad single peak appears in the tanδ curve of PA hydrogel at the frequency 10^{-2} rad/s, in between the two frequencies for the two tanδ peaks of PIC hydrogel, indicating that there is no distinct phase separation of PA hydrogel. The tanδ value of PIC hydrogel is higher than that of PA hydrogel over the wide frequency range except at the high frequency end, indicating the relatively stronger viscoelasticity of the PIC system than that of the PA system.

The apparent activation energy E_a of ionic bonds can be determined using the Arrhenius equation, $a_T = Ae^{E_a/RT}$, where a_T is the shift factor, R is the ideal gas constant, and A is a constant.[7] As shown in Figure 4d, the Arrhenius plot of the PIC gel shows two linear regions with a reflection point at c.a. 50 ℃, giving two activation energies E_a: 62 kJ/mol at high temperature region and 302 kJ/mol at low temperature region, corresponding to 25 k_BT and 121 k_BT (in relative to the room temperature), respectively. The activation energy at low temperature is less than, but close to, the covalent bond dissociation energy, $E_{c\text{-}c} \sim 347$ kJ/mol ($\sim 140\ k_BT$). This explains why a rigid and tough gel is observed even without any covalent cross-linker below the softening temperature. The shift factor a_T

behaviours of the PIC system is very similar to that of the PA hydrogels that also show two activation energies, 71 kJ/mol and 308 kJ/mol above and below the softening temperature. [28] Although the primary structure of the PIC hydrogels and PA hydrogels are completely different, the quite similar shift factor a_T of the two systems suggests that the ionic bond strengths at short molecular scale are similar. Accordingly, the difference of the mechanical behaviors of the two systems comes from the difference in more large scale structure. This is reasonable since both inter-chain and intra-chain bonding exist in PA gels but only inter-chain bonding exists in PIC gels. The latter should have more topological entanglement.

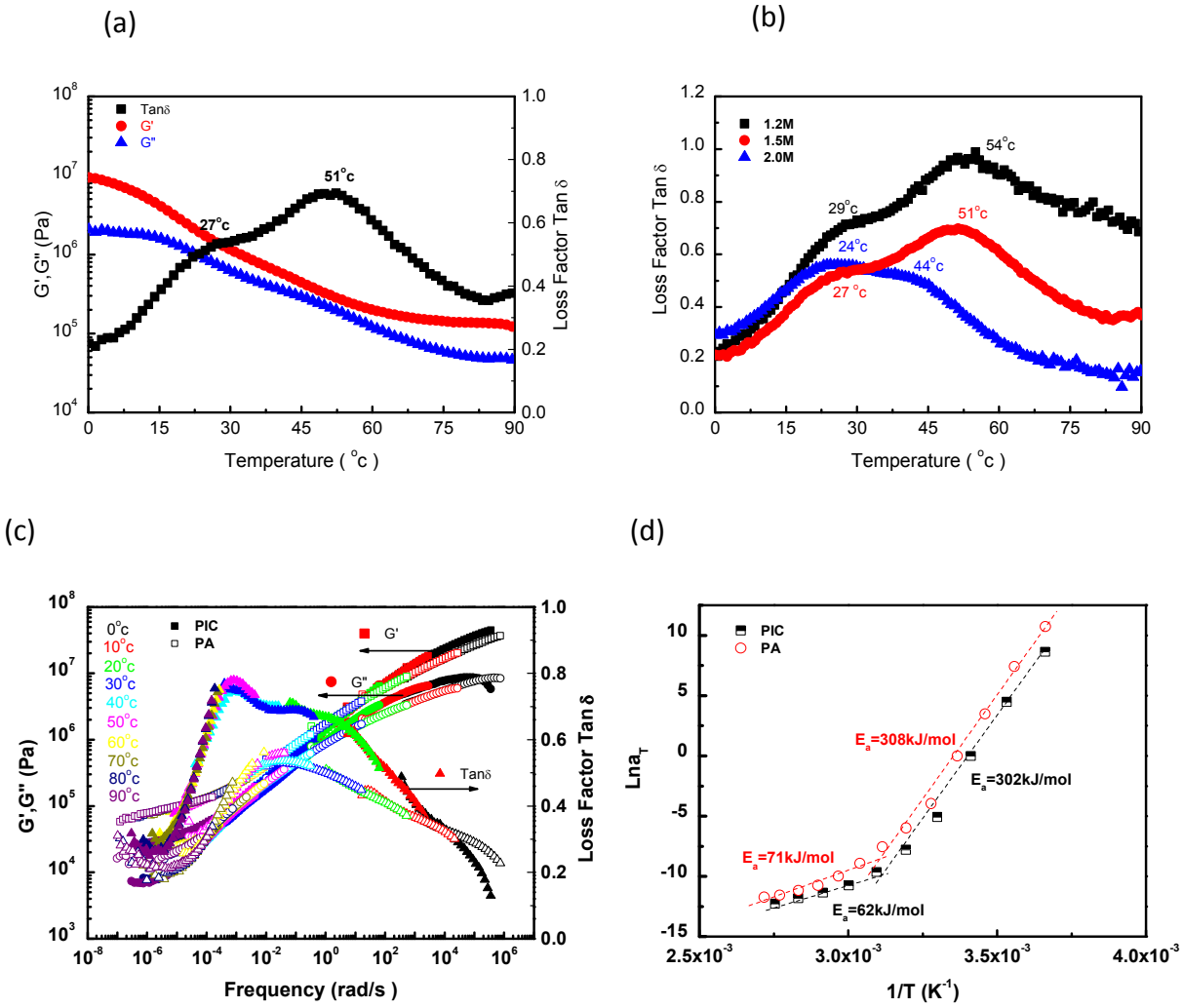


Figure 4. Dynamic mechanical behaviours of the PIC hydrogels in comparison with PA hydrogels. (a) Temperature dependence of storage modulus, G', loss modulus, G″, and loss factor, tanδ, of PMPTC/ PNaSS(1.5-0.5-0.05-0.1) hydrogel at 6.28 rad/s and 0.1% strain. A main peak and a shoulder peak appear in the tanδ curve corresponding to two softening temperatures, T_s, which are indicated by the numbers in the figure; (b) comparison of tanδ for samples PMPTC/PNaSS(C_m-0.5-0.05-0.1) prepared at different monomer concentration, C_m. (c) Frequency (ω) dependences of the storage modulus, G', loss modulus, G″, and loss factor, tanδ, of PMPTC/PNaSS(1.5-0.5-0.05-0.1) hydrogel (filled symbols) and P(MPTC-*co*-NaSS) (2.1-0.52) hydrogel (open symbols). The measurements were performed from 0.0628 to 100 rad/s at a shear strain of 0.5% at different temperatures from 0 °C to 90°C, and the results were obtained by performing classical time-temperature superposition shifts at a reference temperature of 20 °C; (d) Arrhenius plot depicting the temperature dependence of the shift factors for the samples. The apparent activation energy values, E_a, were calculated from the slopes of the curves. The data of P(MPTC-*co*-NaSS) hydrogel are cited from ref. 28.

3.3 Structure Analysis by Scanning Electron Microscopy

To further explore the structure, the structure of freeze-dried PIC and PA hydrogels are observed by SEM and the results are shown in Figure 5. For PIC hydrogel, it exhibits large segregated structure with large pores of diameter ranging from 0.5 to 3 μm. Moreover, the dehydrated polymer formed a granular shape with size around 0.5 μm, suggesting that many chains tightly pack to form a globular structure via the inter-chain ionic bonds. On the other hand, PA hydrogel shows more homogenous structure with

network of a relatively smaller size ranging from 0.1 to 0.3 μm. These results are in good agreement with the rheological measurements that show two relaxation peaks of the PIC hydrogels and single but broad relaxation peak for PA hydrogels.

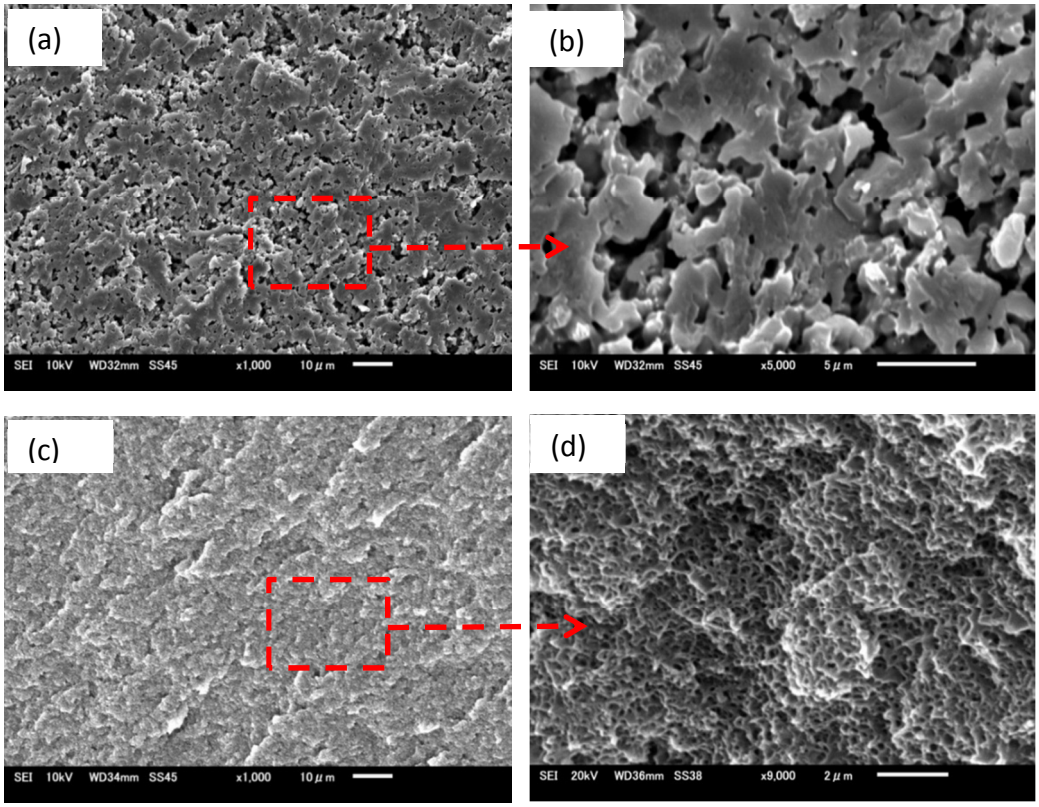


Figure 5. SEM photographs of microstructure of the PIC and PA hydrogels. (a) PMPTC/PNaSS (1.5-0.5-0.05-0.1) hydrogel; (b) The magnification of the zone in (a); (c) P(MPTC-*co*-NaSS) (2.0-0.52) hydrogel; (d) The magnification of the zone in (c).

3.4 Viscoelastic behaviors at large deformation

To ascertain the nonlinear and viscoelastic behavior of the PIC hydrogels at large deformation, we performed uniaxial stretching experiments at various strain rates for the sample of PMPTC/PNaSS (1.5-0.51-0.05-0.1). The tensile stress-strain curves (nominal stress, σ, vs nominal strain, ε) are plotted in Figure 6a. The corresponding data from the

curves are listed in Table 3. The mechanical properties are strongly influenced by strain rate. Yielding is clearly observed around $\varepsilon = 0.5$, and the yield stress, σ_y, increases from 0.08 MPa to 0.69 MPa, as the strain rate increases from 0.0014 to 0.14 s^{-1}. The fracture stress, σ_b, also increases with the strain rate from 0.47 MPa to 3.2 MPa, while the fracture strain decreases slightly. The Young's modulus, E, of samples notably increases about 15 times from 0.34 MPa at 0.0014 s^{-1} to 5.13 MPa at 0.14 s^{-1}. We can see that the strain rate-dependent property for PIC hydrogels are similar to that of PA hydrogels.[29]

According to a recent report by Mayumi et al., the effects of strain and time can be separated for a polyvinyl alcohol (PVA) hydrogel with dual cross-linking, one is permanent, chemical crosslinking, and the other is reversible, physical crosslinking.[36] Similar strain-time separation was observed for the PA hydrogels at low strain rate. [29] Here, we also plot the reduced stress, $\sigma^*=\sigma/(\lambda-\lambda^{-2})$, against the stretching time, t, where $\lambda=\varepsilon+1$ is the stretching ratio. As shown in Figure 6b, $\sigma^*(t)$ shows a decreasing trend with t except for the strain hardening regimes where the reduced stress increases rapidly with time. This indicates that the physical PIC hydrogels behaves as dually cross-linked hydrogels, containing permanent cross-linking (strong bonds) and breakable cross-linking (weak bonds) during deformation. The $\sigma^*(t) \sim t$ curves measured at relatively low stretching rate (0.0014 s^{-1}, 0.007 s^{-1}) overlap, exhibiting a master curve with a slope close to -0.6. This indicates that the strain-time separation is also applicable to PIC hydrogels at low stretching rate, and strain/strain rate have no influence on the breakage rate of the reversible weak bonds. However, at high strain rate (0.014 s^{-1} or higher), the $\sigma^*(t) \sim t$ curves deviate below the master curve, indicates that the high strain rate accelerate the breakage rate of the weak bonds to give a low stress. The strain rate limit of 0.007s^{-1} for

holding the strain-time separation principle is in reasonable agreement with one of the two relaxation peaks at low frequency side (5×10^{-3} rad/s) in Figure 4c. This indicates that the strain-time separation principle is hold when the stretching rate is slower than the inverse of the weak bond breaking time.

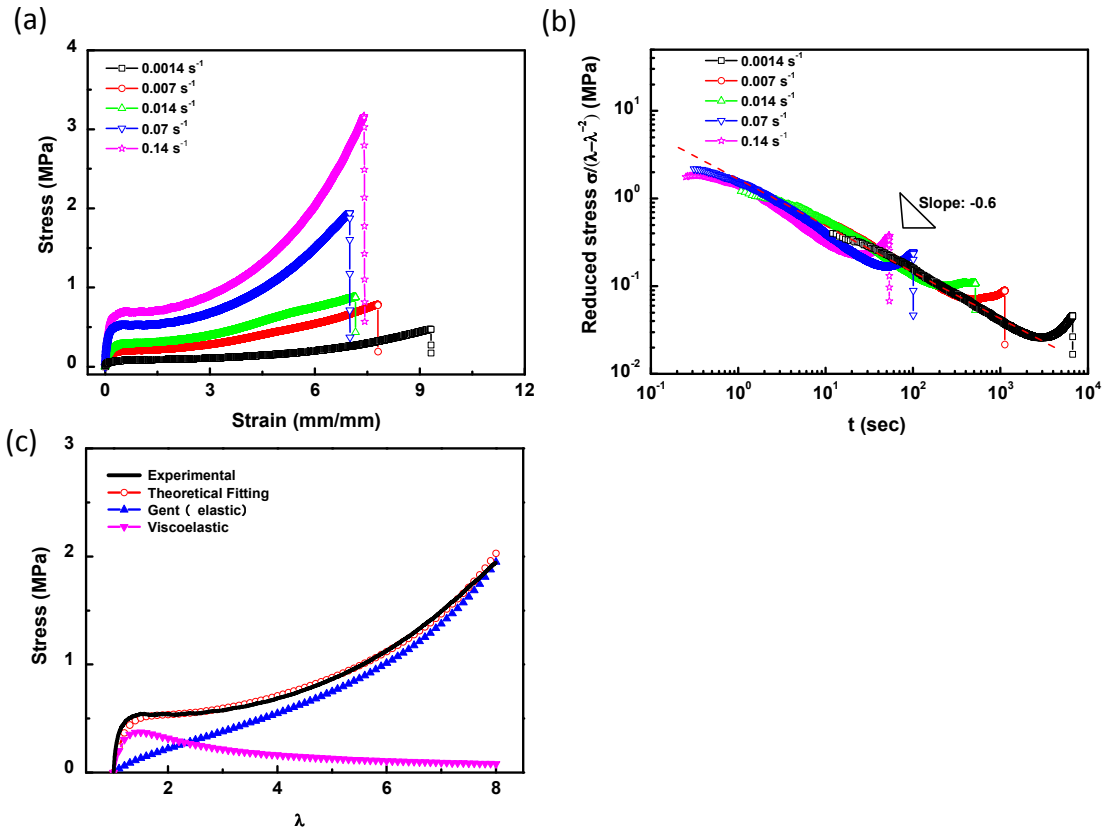


Figure 6. (a) Tensile stress−strain curves for the PMPTC/PNaSS(1.5-0.51-0.05-0.1) hydrogel at various strain rates; (b) Time dependence of the reduced stress $\sigma^*=\sigma/(\lambda-\lambda^{-2})$ at various strain rates, the slope of dash line is -0.6; (c) Typical tensile behaviour at 0.07 s^{-1} (experimental data), and simulated sum of contribution (theoretical fitting curve), and their individually contributions from the viscoelastic part and elastic part (Gent).

Table 3. Summary of the tensile test properties of PMPTC/PNaSS(1.5-0.51-0.05-0.1) hydrogel measured at various stretch rates.

Stretch rate (s^{-1})	E (MPa)*	ε_b	σ_y (MPa)	σ_b (MPa)	G_v (MPa)	D_e	G_e (MPa)	J_m	λ_m	G_v/G_e
0.0014	0.34	9.3	0.08	0.47	0.093	0.243	0.020	177.1	13.4	4.6
0.007	1.08	7.8	0.2	0.78	0.303	0.178	0.057	212.5	14. 7	5.3
0.014	1.59	7.2	0.28	0.88	0.447	0.163	0.083	282.5	16.9	5.4
0.07	3.14	7.0	0.54	1.93	0.923	0.177	0.124	124.5	11.3	7.5
0.14	5.13	7.5	0.69	3.17	1.541	0.136	0.169	122.7	11.2	9.1

* Young's modulus, E, fracture strain, ε_b, yield stress, σ_y, and fracture stress, σ_b, are obtained from the experimental tensile stress-strain curves; shear modulus of the viscoelastic part, G_v, Deborah number, D_e, shear modulus of the elastic part, G_e, the maximum allowable value of the first strain invariant, J_m, and theoretical finite extensibility, λ_m, are obtained from theoretical fitting by equation (1) to (4).

The tensile behaviour of the PIC hydrogels can be further analysed by the viscoelastic model proposed by Creton et al.,[37] which was a parallel combination of the Upper Convected Maxwell (UCM) model for the description of viscoelastic flow and the Gent strain hardening model for the entropic elasticity of finite extensibility of polymer chains. This model can capture the physical features of the viscoelastic phase from the dynamic weak ionic bonds and elastic phase from the strong bonds serving as permanent crosslinkers. The model was used to analyse the viscoelasticity of PA hydrogel system.[33] Herein, we also use this model to analyse the PIC hydrogels. The sum of contributions to the stress, σ_N, from the UCM element and the Gent element can be described as, [37]

$$\sigma_N(\lambda) = \sigma_{N,v}(\lambda) + \sigma_{N,e}(\lambda) \quad \ldots\ldots (1)$$

where

$$\sigma_{N,v}(\lambda) = \left(\frac{2G_vD_e}{1-2D_e}\left(1-\exp\left(-\frac{(1-2D_e)}{D_e}(\lambda-1)\right)\right) + \frac{G_vD_e}{1+D_e}\left(1-\exp\left(-\frac{(1+D_e)}{D_e}(\lambda-1)\right)\right)\right)\lambda^{-1} \ldots\ldots (2)$$

for the viscoelastic stress and

$$\sigma_{N,e}(\lambda) = \left(\frac{G_e}{1-\frac{\lambda^2+2\lambda^{-1}-3}{J_m}}(\lambda^2-\lambda^{-1})\right)\lambda^{-1} \quad \ldots\ldots (3)$$

for the entropic elastic stress, where G_v is the initial shear modulus of the viscoelastic part, D_e is the Deborah number (the product of the relaxation time of the viscous component and the strain rate), G_e is the shear modulus at small strain from the elastic part, and λ is the elongation ratio ($\lambda = \varepsilon + 1$). J_m is the maximum allowable value of the first strain invariant, and it is related to the theoretical finite extensibility of the network chains λ_m as,

$$J_m = \lambda_m^2 + 2\lambda_m^{-1} - 3 \ldots\ldots (4)$$

Eq. 1 is determined by four parameters G_e, λ_m, G_v, and D_e. Since the Young's modulus $E = 3(G_e + G_v)$, we can fit the tensile stress-strain data with the model using three independent parameters and the Young's modulus E estimated from the tensile behaviour. A representative stress-elongation curve for the PIC hydrogel as well as simulated curves of the two individual contributions to the tensile behavior is presented in Figure 6c. A good fit by such a combined model to the tensile data of PIC gels can be obtained. A systematic fitting to the tensile behavior of hydrogels in different tensile rates are performed to understand how the ionic bonds affect the mechanical behavior of the hydrogels, and the related simulated parameters are shown in Table 3. The Deborah

number, D_e, in the fitting serves as the adjusting parameter. An importantant parameter, G_v/G_e, characterizes the ratio of polymer chains crosslinked by temporary weak bonds and quasi-permanent strong bonds. The value of G_v/G_e also indicates the average number of weak bonds between two neighbouring strong bonds.[37] Therefore, it is an assessment of the degree of viscoelastic characters and how much energy dissipates occurs during deformation, contributing to toughness. It is clearly shown that the G_v/G_e of all the samples increase with the acceleration of stretch rate, which is consistent with the typical viscoelastic character of PIC hydrogel depending on the stretch rate. In comparison with PA system, the G_v/G_e of the PIC system is high, which is in agreemet with the dynamic rheological results (Figure 4c). [33] Furthermore, the theoretical finite extensibility of the network chains λ_m of the PIC hydrogel at low strain rate ($\lambda_m \sim 13$) is much smaller than that of the PA hydrogel ($\lambda_m \sim 18$).[33] This could be related to the stronger entanglement of the PIC system than that of the PA system, as discussed in the previous section.

4. Conclusion

As like the PA hydrogels, the most strong and tough PIC hydrogels are formed near the equal charge ratio and the PIC hydrogels show strong viscoelastic character with wide ionic bonds distribution. For PA hydrogels, the opposite charges, randomly dispersed along the polymer chains, form ionic bonds of a wide strength distribution through inter-chain and intra-chain complexation. The polyelectrolyte chains are in globule conformation due to intra-chain ionic bonds even at the preparation state, in the presence of large amount of small ions. Because of this, the inter-chain ionic bonds that contribute to the elasticity of the gels could only be formed at extremely high preparation concentration (C_m > 1.3 M). They show substantial swelling and low modulus at low

polymer concentration due to poor entanglement between chains (C_m<1.6 M). On the other hand, for PIC hydrogels, the homo-charged polymers in the as-prepared state take relatively extended coil conformation because the like-charged segments repel each other and no intra-chain ionic bonds could be formed. This greatly favors the chain entanglement even at relatively low polymer concentration C_m (> 0.2 M). By dialysis of the sample in water, the mobile small ions are removed from the gel, and inter-chain complexation between entangled, oppositely charged polymers is formed. Thus, tough PIC gels can be formed at very low concentration C_m. Although the primary structure of the PIC hydrogels and PA hydrogels are completely different, the activation energies, which are the energy barriers of the local motion, of the two systems are quite similar. This means that, that the ionic bond strengths at short molecular scale are similar for the two systems. Accordingly, the difference of the mechanical behaviors of the two systems comes from the difference in more large scale structure. SEM observation of the samples morphology supports this argument. The PA shows more uniform structure with small pore size, while the PIC shows a more inhomogeneous, segregated porous structure with large pore size. These differences in large scale structure seem to dominant the bulk mechanical properties of the two systems. On the basis of the different structural character between PA gels and PIC gels, PIC gels possess several advantages such as less C_m-dependence, easy reprocessability, and strong self-glued ability.[31-32]

Acknowledgements

This research was financially supported by Grant-in-Aid for Scientific Research (S) (No. 124225006) and for Postdoctoral Fellowships for Foreign Researchers (No. P12340)

from the Japan Society for the Promotion of Science (JSPS). This research was also funded by ImPACT Program of Council for Science, Technology and Innovation (Cabinet Office, Government of Japan).

References

1. Sun, J. Y.; Zhao, X. H.; Illeperuma, W. R. K.; Chaudhuri, O.; Oh, K. H.; Mooney, D. J.; Vlassak, J. J.; Suo, Z. G., *Highly stretchable and tough hydrogels*. *Nature* **2012,** *489* (7414), 133-136.
2. Peppas, N. A.; Hilt, J. Z.; Khademhosseini, A.; Langer, R., *Hydrogels in biology and medicine: from molecular principles to bionanotechnology*. *Adv. Mater.* **2006,** *18* (11), 1345-1360.
3. Nowak, A. P.; Breedveld, V.; Pakstis, L.; Ozbas, B.; Pine, D. J.; Pochan, D.; Deming, T. J., *Rapidly recovering hydrogel scaffolds from self-assembling diblock copolypeptide amphiphiles*. *Nature* **2002,** *417* (6887), 424-428.
4. Calvert, P., *Hydrogels for soft machines*. *Adv. Mater.* **2009,** *21* (7), 743-756.
5. Zhao, X., *Multi-scale multi-mechanism design of tough hydrogels: building dissipation into stretchy networks*. *Soft Matter* **2014,** *10* (5), 672-687.
6. Kim, J.; Hanna, J. A.; Byun, M.; Santangelo, C. D.; Hayward, R. C., *Designing responsive buckled surfaces by halftone gel lithography*. *Science* **2012,** *335* (6073), 1201-1205.
7. Henderson, K. J.; Shull, K. R., *Effects of Solvent Composition on the Assembly and Relaxation of Triblock Copolymer-Based Polyelectrolyte Gels*. *Macromolecules* **2012,** *45* (3), 1631-1635.
8. Li, J.; Illeperuma, W. R.; Suo, Z.; Vlassak, J. J., *Hybrid Hydrogels with Extremely High Stiffness and Toughness*. *Acs Macro Lett.* **2014,** *3*, 520-523.
9. Gong, J. P.; Katsuyama, Y.; Kurokawa, T.; Osada, Y., *Double‐Network Hydrogels with Extremely High Mechanical Strength*. *Adv. Mater.* **2003,** *15* (14), 1155-1158.
10. Wang, J.; Lin, L.; Cheng, Q.; Jiang, L., *A Strong Bio‐Inspired Layered PNIPAM‐Clay Nanocomposite Hydrogel*. *Angewandte Chemie* **2012,** *124* (19), 4754-4758.
11. Schexnailder, P.; Schmidt, G., *Nanocomposite polymer hydrogels*. *Colloid Polym. Sci.* **2009,** *287* (1), 1-11.
12. Yang, C. H.; Wang, M. X.; Haider, H.; Yang, J. H.; Sun, J.-Y.; Chen, Y. M.; Zhou, J.; Suo, Z., *Strengthening alginate/polyacrylamide hydrogels using various multivalent cations*. *ACS Appl. Mater. Inter.* **2013,** *5* (21), 10418-10422.
13. Lin, P.; Ma, S.; Wang, X.; Zhou, F., *Molecularly Engineered Dual‐Crosslinked Hydrogel with Ultrahigh Mechanical Strength, Toughness, and Good Self‐Recovery*. *Adv. Mater.* **2015,** *27* (12), 2054-2059.
14. Xia, L.-W.; Xie, R.; Ju, X.-J.; Wang, W.; Chen, Q.; Chu, L.-Y., *Nano-structured smart hydrogels with rapid response and high elasticity*. *Nat.Commun.* **2013,** *4*, 2226.
15. Huang, T.; Xu, H.; Jiao, K.; Zhu, L.; Brown, H. R.; Wang, H., *A novel hydrogel with high mechanical strength: a macromolecular microsphere composite hydrogel*. *Adv. Mater.* **2007,** *19* (12), 1622-1626.
16. Gong, J. P., *Why are double network hydrogels so tough? Soft Matter* **2010,** *6* (12), 2583-2590.

17. Cordier, P.; Tournilhac, F.; Soulié-Ziakovic, C.; Leibler, L., *Self-healing and thermoreversible rubber from supramolecular assembly*. *Nature* **2008,** *451* (7181), 977-980.
18. Burnworth, M.; Tang, L.; Kumpfer, J. R.; Duncan, A. J.; Beyer, F. L.; Fiore, G. L.; Rowan, S. J.; Weder, C., *Optically healable supramolecular polymers*. *Nature* **2011,** *472* (7343), 334-337.
19. Henderson, K. J.; Zhou, T. C.; Otim, K. J.; Shull, K. R., *Ionically cross-linked triblock copolymer hydrogels with high strength*. *Macromolecules* **2010,** *43* (14), 6193-6201.
20. Hunt, J. N.; Feldman, K. E.; Lynd, N. A.; Deek, J.; Campos, L. M.; Spruell, J. M.; Hernandez, B. M.; Kramer, E. J.; Hawker, C. J., *Tunable, high modulus hydrogels driven by ionic coacervation*. *Adv. Mater.* **2011,** *23* (20), 2327-2331.
21. Chassenieux, C.; Tsitsilianis, C., *Recent trends in pH/thermo-responsive self-assembling hydrogels: from polyions to peptide-based polymeric gelators*. *Soft Matter* **2016,** *12*, 1344-1359.
22. Dyakonova, M.; Stavrouli, N.; Popescu, M.; Kyriakos, K.; Grillo, I.; Philipp, M.; Jaksch, S.; Tsitsilianis, C.; Papadakis, C., *Physical Hydrogels via Charge Driven Self-Organization of a Triblock Polyampholyte–Rheological and Structural Investigations*. *Macromolecules* **2014,** *47* (21), 7561-7572.
23. Lemmers, M.; Sprakel, J.; Voets, I. K.; van der Gucht, J.; Stuart, C.; Martien, A., *Multiresponsive Reversible Gels Based on Charge‐Driven Assembly*. *Angewandte Chemie* **2010,** *122* (4), 720-723.
24. Gao, H.; Yao, H., *Shape insensitive optimal adhesion of nanoscale fibrillar structures*. *P. Natl. Acad. Sci. USA* **2004,** *101* (21), 7851-7856.
25. Burattini, S.; Colquhoun, H. M.; Fox, J. D.; Friedmann, D.; Greenland, B. W.; Harris, P. J.; Hayes, W.; Mackay, M. E.; Rowan, S. J., *A Self-repairing, supramolecular polymer system: healability as a consequence of donor–acceptor π–π stacking interactions*. *Chem. Commun.* **2009,** (44), 6717-6719.
26. Hao, J.; Weiss, R., *Viscoelastic and mechanical behavior of hydrophobically modified hydrogels*. *Macromolecules* **2011,** *44* (23), 9390-9398.
27. Haque, M. A.; Kurokawa, T.; Kamita, G.; Gong, J. P., *Lamellar bilayers as reversible sacrificial bonds to toughen hydrogel: hysteresis, self-recovery, fatigue resistance, and crack blunting*. *Macromolecules* **2011,** *44* (22), 8916-8924.
28. Sun, T. L.; Kurokawa, T.; Kuroda, S.; Ihsan, A. B.; Akasaki, T.; Sato, K.; Haque, M. A.; Nakajima, T.; Gong, J. P., *Physical hydrogels composed of polyampholytes demonstrate high toughness and viscoelasticity*. *Nat. Mater.* **2013,** *12* (10), 932-937.
29. Luo, F.; Sun, T. L.; Nakajima, T.; Kurokawa, T.; Zhao, Y.; Ihsan, A. B.; Guo, H. L.; Li, X. F.; Gong, J. P., *Crack Blunting and Advancing Behaviors of Tough and Self-healing Polyampholyte Hydrogel*. *Macromolecules* **2014,** *47*, 6037-6046.
30. Ihsan, A. B.; Sun, T. L.; Kuroda, S.; Haque, M. A.; Kurokawa, T.; Nakajima, T.; Gong, J. P., *A phase diagram of neutral polyampholyte–from solution to tough hydrogel*. *J. Mater. Chem. B* **2013,** *1* (36), 4555-4562.
31. Luo, F.; Sun, T. L.; Nakajima, T.; Kurokawa, T.; Zhao, Y.; Sato, K.; Ihsan, A. B.; Li, X.; Guo, H.; Gong, J. P., *Oppositely Charged Polyelectrolytes Form Tough, Self‐Healing, and Rebuildable Hydrogels*. *Adv. Mater.* **2015,** *27* (17), 2722-2727.

32. Luo, F.; Sun, T. L.; Nakajima, T.; Kurokawa, T.; Ihsan, A. B.; Li, X.; Guo, H.; Gong, J. P., *Free Reprocessability of Tough and Self-Healing Hydrogels Based on Polyion Complex*. *Acs Macro Lett.* **2015,** *4*, 961-964.
33. Sun, T. L.; Luo, F.; Kurokawa, T.; Karobi, S. N.; Nakajima, T.; Gong, J. P., *Molecular structure of self-healing polyampholyte hydrogels analyzed from tensile behaviors*. *Soft Matter* **2015,** *11*, 9355-9366.
34. Klein, J. W., A., *J. Polym. Sci., Polym. Chem. Ed.* **1981,** *19*, 707.
35. Dobrynin, A. V.; Colby, R. H.; Rubinstein, M., *Scaling theory of polyelectrolyte solutions*. *Macromolecules* **1995,** *28* (6), 1859-1871.
36. Mayumi, K.; Marcellan, A.; Ducouret, G.; Creton, C.; Narita, T., *Stress–Strain Relationship of Highly Stretchable Dual Cross-Link Gels: Separability of Strain and Time Effect*. *Acs Macro Lett.* **2013,** *2* (12), 1065-1068.
37. Deplace, F.; Rabjohns, M. A.; Yamaguchi, T.; Foster, A. B.; Carelli, C.; Lei, C. H.; Ouzineb, K.; Keddie, J. L.; Lovell, P. A.; Creton, C., *Deformation and adhesion of a periodic soft-soft nanocomposite designed with structured polymer colloid particles*. *Soft Matter* **2009,** *5* (7), 1440-1447.